Asaf Marco,[1,2] Tatiana Kisliouk,[3] Tzlil Tabachnik,[1,2] Aron Weller,[2,4] and Noam Meiri[3]

DNA CpG Methylation (5-Methylcytosine) and Its Derivative (5-Hydroxymethylcytosine) Alter Histone Posttranslational Modifications at the *Pomc* Promoter, Affecting the Impact of Perinatal Diet on Leanness and Obesity of the Offspring

Diabetes 2016;65:2258–2267 | DOI: 10.2337/db15-1608

OBESITY STUDIES

A maternal high-fat diet (HFD) alters the offspring's feeding regulation, leading to obesity. This phenomenon is partially mediated by aberrant expression of the hypothalamic anorexigenic neuropeptide proopiomelanocortin (POMC). Nevertheless, although some individual offspring suffer from morbid obesity, others escape the malprogramming. It is suggested that this difference is due to epigenetic programming. In this study, we report that in lean offspring of non-HFD–fed dams, essential promoter regions for *Pomc* expression were enriched with 5-hydroxymethylcytosine (5hmC) together with a reduction in the level of 5-methylcytosine (5mC). Moreover, 5hmC was negatively correlated whereas 5mC was positively correlated with body weight in offspring from both HFD- and control-fed dams. We further found that *Pomc* expression in obese offspring is determined by a two-step epigenetic inhibitory mechanism in which CpG methylation is linked with histone posttranslational modifications. An increase in CpG methylation at the *Poxmc* promoter enables binding of methyl-binding domain 1 (MBD1) to 5mC, but not to its derivative 5hmC. MBD1 then interacts with SET domain bifurcated 1 methyltransferase to promote bimethylation on the histone 3 lysine 9 residue, reducing *Pomc* mRNA expression. These results suggest an epigenetic regulatory mechanism that affects obesity-prone or resilient traits.

A maternal high-fat diet (HFD) affects the offspring's intake regulation, leading, in some cases, to obesity. It has been suggested that this phenomenon is at least partially mediated by epigenetic malprogramming of hypothalamic anorexigenic neuropeptides, such as proopiomelanocortin (POMC) (1–3).

Epigenetic processes comprise several regulatory layers, including DNA and histone modifications, which remodel chromatin and thereby activate or silence genes without changing the genomic DNA sequence (4). DNA is preferentially modified by adding a methyl group to the cytosine on CpG (cytosine–guanine) dinucleotides, producing 5-methylcytosine (5mC) (5). Recently, a dynamic DNA epigenetic regulatory network comprising three additional cytosine variants was identified. These cytosine derivatives were produced from stepwise oxidation of 5mC by the ten-eleven translocation family of dioxygenase enzymes (6). One of these derivatives, 5-hydroxymethylcytosine (5hmC), was shown to be enzymatically produced in relatively high abundance in brain tissues, where it is suspected to play a regulatory role in neurodevelopment as well as in neurological diseases (7). Moreover, 5hmC can be used as a stable epigenetic mark that is enriched in active genes, facilitating transcription through its effects on chromatin organization (8).

[1]Faculty of Life Sciences, Bar Ilan University, Ramat-Gan, Israel
[2]Department of Psychology, Bar Ilan University, Ramat-Gan, Israel
[3]Institute of Animal Science, Agricultural Research Organization, The Volcani Center, Bet Dagan, Israel
[4]Gonda Multidisciplinary Brain Research Center, Bar Ilan University, Ramat-Gan, Israel

Corresponding author: Noam Meiri, meiri@agri.huji.ac.il.

Received 24 November 2015 and accepted 27 April 2016.

A second regulatory step that affects chromatin structure and accessibility is determined by histone posttranslational modifications (PTMs) (4). These marks modify the local electrochemical properties of chromatin, altering its conformation and thereby regulating the accessibility of genes to the transcriptional machinery.

New evidence shows an interaction between DNA and histone modifications mediated through methyl-binding domain (MBD) proteins (9). The MBD proteins, namely MeCP2 and MBD1–4, bind to methylated CpG sequences and recruit enzymatic machinery such as histone deacetylases (HDACs), suppressor of variegation 3–9 homolog 1 (SUV39H1), and other chromatin-remodeling complexes affecting transcription regulators.

The hypothalamic arcuate (ARC) nucleus regulates eating behavior and energy balance (10). It contains two sets of neurons: the Agouti-related peptide/neuropeptide Y (AgRP/NPY) neurons that stimulate food intake and decrease energy expenditure, and POMC/cocaine- and amphetamine-regulated transcript neurons that inhibit food intake. These neurons respond to circulating peripheral hormones such as insulin, leptin, and ghrelin, which represent the status of the body's energy stores (10). The gene encoding POMC produces several different posttranscriptional cleavage products, one of which is the appetite suppressor neuropeptide α–melanocyte-stimulating hormone, which is crucially involved in body weight (BW) control (11). Therefore, "aberrant" epigenetic modifications can affect normal *Pomc* expression, leading to obesity. Exposure to maternal HFD-induced obesity increases BW and food intake in the offspring, which is accompanied by increased methylation at the *Pomc* locus (1–3). We now report that 5mC and 5hmC have different roles in regulating the expression of *Pomc* in the hypothalamic ARC nucleus by establishing different complexes that modify chromatin structure.

RESEARCH DESIGN AND METHODS

Animals

Wistar rats supplied by Harlan Laboratories (Jerusalem, Israel) were raised at Bar-Ilan University. Females were raised from postnatal day (PND) 22 to PND80 on either HFD or chow (C), then mated, and the offspring were studied. Standard chow (2018SCF Teklad Global 18% protein 6% fat rodent diet; Harlan Laboratories, Madison, WI) or HFD (D12492, rodent diet with 60% fat; Research Diets Inc.) was freely available. Food intake was converted to kilocalories as: 1 g C diet = 3.1 kcal and 1 g HFD = 5.24 kcal. The animals were on a 12:12 h light/dark cycle. Litter size was adjusted on PND1 to 8–10. The research was approved by the Institutional Animal Care and Use Committee and adhered to the guidelines of the Society for Neuroscience.

Brain Sections

Frozen coronal brain sections were cut using a cryostat (−2.12 to −4.5 mm from the bregma according to Paxinos and Watson), and ARC punches were either immersed in RNALater (Ambion, Austin, TX) or frozen in dry ice.

RNA Isolation and Real-Time PCR

RNA was isolated and reverse-transcribed as previously described (12). Hypoxanthine phosphoribosyltransferase 1 (*Hprt1*) and β_2 microglobulin (*B2m*) were used as reference genes for quantitative RT-PCR. The primers were (5′→3′): *Pomc* forward (F), GCTACGGCGGCTTCATGA and *Pomc* reverse (R), CCTCACTGGCCCTTCTTGTG; Npy F, TC CTAGTTTCCCCCCACATCT and Npy R, AAGGGAAATGGGT CGGAATC; AgRp F, AAGCTTTGGCAGAGGTGCTA and AgRp R, ACTCGTGCAGCCTTACACA; Hprt1 F, GCGAAAGTGGAA AAGCCAAGT and Hprt1 R, GCCACATCAACAGGACTCT TGTAG; and B2m F, TTCCACCCACCTCAGATAGAAAT and B2m R, TGTGAGCCAGGATGTAGAAAGAC.

Chromatin Immunoprecipitation–Quantitative PCR Analysis

This analysis was performed using SimpleChIP Chromatin IP Kit (Cell Signaling Technology) with antibodies anti-MBD1 (Epigentek, Farmingdale, NY), anti-MeCP2 (Santa Cruz Biotechnology, Santa Cruz, CA), anti–histone 3 lysine 9 residue (H3K9me2; Millipore, Darmstadt, Germany), anti-H3K9me3 (Millipore), and anti-IgG (1:3,000; Cell Signaling Technology) as a negative control. DNA was isolated from each immunoprecipitate and subjected to real-time PCR with primers (5′→3′): *Pomc* F, CCTCACACCAGGATGC TAAGC and *Pomc* R, CAGCAGATGTGCCTGGAAAG; and exon 3 F, GCTACGGCGGCTTCATGA and exon 3 R, CCTC ACTGGCCCTTCTTGTG. Immunoprecipitated DNA is presented as a signal relative to 1% of the total amount of input chromatin.

Western Blotting

This protocol was the same as reported previously (1), using primary antibodies anti-MBD1 (1:500; Epigentek), anti-SETDB1 (1:200; Bioss, Woburn, MA), and anti–β-actin (1:2,000; Cell Signaling Technology). The secondary antibody was anti-rabbit IgG horseradish peroxidase–conjugated antibody (1:3,000; Amersham Biosciences, Little Chalfont, U.K.).

Coimmunoprecipitation

ARC nucleus samples were homogenized on ice with 500 μL lysis buffer (25 mmol/L Tris HCl, 150 mmol/L NaCl, 1 mmol/L EDTA, 1% Nonidet P-40, and 5% glycerol and protease inhibitor cocktail). A homogenized sample was used as the input control. Homogenates were immunoprecipitated with anti-MBD1 (Epigentek), anti-SETDB1 (Bioss), anti-5hmC (Active Motif, Carlsbad, CA), or anti-5mC (Abcam, Cambridge, U.K.) antibodies overnight. Antigen–antibody complexes were separated with Pierce protein A/G magnetic beads. Immunoprecipitated samples and their inputs were subjected to Western blot.

5mC and 5hmC Analysis

For DNA oxidation, purified DNA from the hypothalamic ARC nucleus of weanling offspring of chow- and HFD-fed mothers (C-C and HFD-C, respectively) was denatured in

0.05 mol/L NaOH for 30 min at 37°C. Then 1 μL of 15 mmol/L $KRuO_4$ in 0.05 mol/L NaOH was added to the denatured DNA for 1 h on ice. Oxidized DNA was purified by ethanol/LiCl precipitation and dissolved in water.

Bisulfite Modification

Both untreated DNA and oxidized DNA samples were converted by bisulfite treatment using Imprint DNA Modification kit (Sigma-Aldrich, St. Louis, MO). For methylation analysis, *Pomc* promoter was amplified with primer pair F, 5′-GTTTTGGGTTGTTATGATTTTTGAT-3′ and R, 5′-AATCCCTATCACTCTTCTCTCTT-3′. The PCR products were cloned into PGEMT-easy vectors (Promega, Madison, WI), inserted into JM109 competent *Escherichia coli* cells (Promega), and purified with the QIAprep Spin Miniprep kit (Qiagen). *Pomc* promoter was analyzed by sequencing (Macrogene, Seoul, Korea), and the percentage of 5mC and 5hmC was measured from 12 to 17 clones per rat.

Immunofluorescent Staining

Frozen coronal brain sections were cut using a cryostat (−2.12 to −4.5 mm from bregma). Sections were fixed with 4% paraformaldehyde, washed with Tris-buffered saline (TBS), and frozen. Slides were blocked in 5% donkey serum and 1% BSA. The sections were double-immunostained with anti-H3K9me2 (1:100; Millipore) and anti-POMC (1:50; Abcam) antibodies overnight at 4°C. After three TBS washes, slides were incubated with Alexa Fluor 488 goat anti-rabbit IgG (1:500; Invitrogen Molecular Probes, Eugene, OR) as a secondary antibody for anti-H3K9me2 and Alexa Fluor 555 goat anti-chicken IgG (1:500; Invitrogen) as a secondary antibody for anti-POMC for 1 h at room temperature. After a TBS wash, slides were counterstained with DAPI (Sigma-Aldrich) and photographed under a fluorescence microscope. Four different sections were examined per slide, 20 slides per rat. At least four different rats were analyzed per treatment. The number of stained cells was analyzed by ImageJ 1.3 image analysis software (National Institutes of Health).

RESULTS

Maternal Chronic HFD Consumption Has a Long-term Effect on Normally Fed Offspring

Normally fed offspring of HFD-fed dams consumed more kilocalories of chow diet than offspring of normally fed mothers at PND25 (HFD-C, $n = 7$, 24.3 ± 0.2 kcal; C-C, $n = 13$, 18.5 ± 0.5 kcal; $P < 0.001$) (Fig. 1*A*). Two months of postweaning normal nutrition did not alter the overeating phenotype of these rats, which continued to display excessive consumption of chow until adulthood ($F_{(1,198)} = 25.27$ for the overall difference between HFD-C and C-C groups, $P = 0.0001$) (Fig. 1*A*). The difference in BW was evaluated at two different time points: weaning and adulthood. At each time point, the control (C-C) group was set to 100%. Offspring of HFD-fed dams (HFD-C) presented greater BW ($P < 0.0001$) than controls on day of weaning (C-C, $n = 13$; HFD-C 88 ± 2.8% difference, $n = 9$) (Fig. 1*B*) and at adulthood (HFD-C, 35 ± 8.8% difference, $P = 0.003$) (Fig. 1*B*). We previously reported (13) that weaned offspring of HFD-treated dams have higher leptin levels than normally fed controls. Although a high leptin signal should enhance the anorexigenic activity of POMC's product α–melanocyte-stimulating hormone, *Pomc* relative mRNA expression was low in these rats ($n = 6$, $P = 0.039$) (Fig. 1*C*). It is worth noting that there were lower levels of both *Npy* and *AgRp* mRNA in the HFD-C group compared with C-C controls ($n = 6$, $P = 0.047$ and $P = 0.034$, respectively) (Fig. 1*C*), indicating that the orexigenic system is responsive to the leptin signal.

Essential Transcription Sites at the *Pomc* Promoter Are Enriched in 5hmC and Have Reduced 5mC Levels in Lean Weaned Offspring

To differentiate between the distribution and levels of 5hmC and 5mC marks on the *Pomc* promoter, the ARC nucleus of weanling offspring was subjected to oxidative bisulfite sequencing (12). Analysis of single CpG sites in the offspring of HFD- and standard chow-fed dams revealed different methylation patterns. The HFD-C had higher total 5mC levels ($P = 0.07$) than their C-C counterparts (Fig. 2*C*), with hypermethylation at sites −202, −192, −166, and −164 bp upstream of the transcriptional start site (Bonferroni post hoc tests, −202, $P = 0.1$; all other sites, $P < 0.05$) (Fig. 2*A*). In contrast, C-C presented higher levels of 5hmC at sites −202, −164, and −115 compared with the heavier HFD-C (Bonferroni post hoc tests, all $P < 0.05$) (Fig. 2*B*). We analyzed the methylation pattern in a specific cluster of seven CpG dinucleotides −192 to −133 bp from the transcriptional start site, which had been previously shown to affect the binding levels of the transcription factors Sp1 and nuclear factor-κB (3). Offspring of HFD-fed dams demonstrated higher 5mC levels in this region compared with the lean offspring ($P = 0.01$) (Fig. 2*D*). Conversely, higher 5hmC levels were observed in the offspring of chow-fed dams compared with the HFD-C group ($P = 0.03$) (Fig. 2*D*). Because the main hypothesis of this study was that different methylation patterns and levels affect weight gain, BW of the rats from both groups was correlated with the levels of 5mC and 5hmC. Negative correlations were found between the BW of individual rats (from both groups) and their 5hmC levels in the −192 to −133 cluster ($r = -0.75$, $P = 0.02$) (Fig. 2*E*). In contrast, 5mC levels and total methylation levels (5mC + 5hmC) were positively correlated with BW ($r = 0.83$, $P = 0.006$ [Fig. 2*F*] and $r = 0.62$, $P = 0.053$ [Fig. 2*G*], respectively).

Chronic HFD Consumption Is Associated With Higher H3K9 Methylation Levels at the *Pomc* Promoter in the Hypothalamic ARC Nucleus

Hypermethylated DNA tends to coexist with histone PTMs such as methyl-H3 on heterochromatic regions (5). In this study, bi- and trimethylation levels of H3K9 and H3K27 were analyzed by quantitative reverse-transcription–chromatin immunoprecipitation (ChIP) assays on the *Pomc* promoter (H3K9me2, H3K9me3, H3K27me2, and H3K27me3, respectively). One-way ANOVA of the results

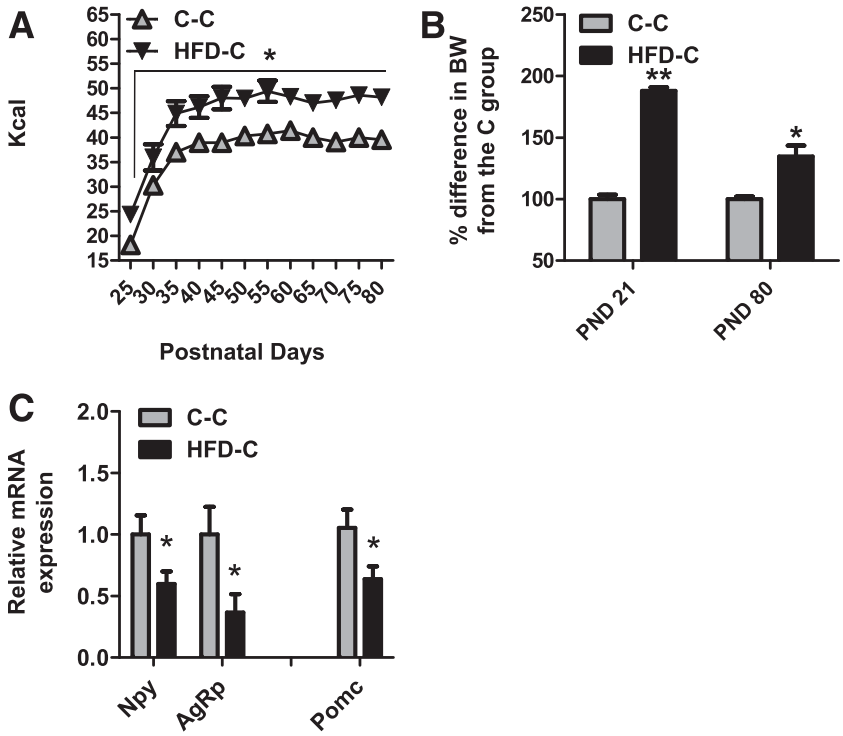

Figure 1—Food consumption, BW, and *Pomc* expression are affected in the offspring by the dam's diet. F0 females were allocated randomly to two groups and raised from PND 22 to PND 80 on either an HFD or C diet. At PND 80, the females were mated with a chow-fed Wistar male (of average weight) to create the next generation. The diet conditions continued through conception, gestation, and lactation. Half of the offspring were euthanized at weaning for analyses, and the rest were raised on chow diet until adulthood. *A*: Food intake was measured every fifth day in grams and converted to kcal (1 g C diet = 3.1 kcal; 1 g HFD = 5.24 kcal), according to the manufacturer's data. *B*: Percent difference in BW was measured in the offspring of HFD-treated dams compared with offspring of C dams, which was set to 100%. Animals were compared at two ages: PND 21 and PND 80. *C*: Offspring of C and HFD dams were sacrificed and analyzed for ARC nucleus mRNA expression levels of *Pomc*, *Npy*, and *AgRp*. Relative gene expression in the C group was set to 1. *Hprt1* and *B2m* were used as standard genes. All data are presented as means ± SEM. $^{*}P < 0.05$, $^{**}P < 0.01$ vs. control group.

from the weanling offspring showed differences between groups in H3K9me2 levels ($F_{(2,14)} = 21.4$; $P = 0.0001$). A Bonferroni post hoc test revealed higher H3K9me2 binding levels on the *Pomc* promoter compared with the control group ($n = 7$, $P = 0.043$) (Fig. 3*A*). IgG was used as a control for nonspecific binding. Bonferroni post hoc tests showed that IgG was different from both groups ($P = 0.001$). To verify the specificity of the ChIP assay to the *Pomc* promoter, an additional site was evaluated at position +5615 to +5714 bp downstream of the transcriptional start site (exon 3). There was no statistical difference between groups at this site (Fig. 3*A*). In addition, there were no statistical differences between the groups in H3K9me3 (Fig. 3*B*) or H3K27me2/me3 on the *Pomc* promoter (data not shown). Pearson product-moment correlations among individual rats' BW and their H3K9 methylation levels at the *Pomc* promoter were performed in weanling offspring from both HFD-C and C-C groups. It was found that beyond the mother's dietary composition, in weanling pups, there was a positive correlation between BW and the H3K9me2 modification ($r_{(12)} = 0.78$; $P = 0.003$) (Fig. 3*C*). To further determine whether the H3K9me2 modification is specifically associated with and located in the hypothalamic ARC POMC neurons, we subjected coronal brain sections from C-C and HFD-C rats to immunofluorescence assay. The brain sections were coimmunostained with anti-H3K9me2 and anti-POMC antibodies and DAPI. Colocalization of all three marks is shown in Fig. 3*D*, indicating that the H3K9me2 mark is present in the nuclei of the POMC neurons. In addition, ImageJ software (National Institutes of Health) was used to quantify three additional parameters: H3K9me2 and POMC abundance in the ARC nucleus, which was determined by the ratio to the DAPI signal (H3K9me2/DAPI and *Pomc*/DAPI, respectively), and the ratio between *Pomc* and H3K9me2 (*Pomc*/H3K9me2). The results, summarized in Fig. 3*E*, show that the HFD-C group had low *Pomc*/DAPI and *Pomc*/H3K9me2 ratios in the ARC nucleus ($P < 0.001$), suggesting that these rats have low *Pomc* expression in the presence of H3K9me2 marks.

MBD1 Interacts With 5mC, but Not With 5hmC, to Promote Repressive Complex and Silence *Pomc* Promoter in HFD-C

It was recently suggested that dual epigenetic silencing marks on the DNA sequence and histone tails are mediated through MBD proteins (14). Hence, to gain further insight into the complexes linking 5mC or 5hmC modifications to

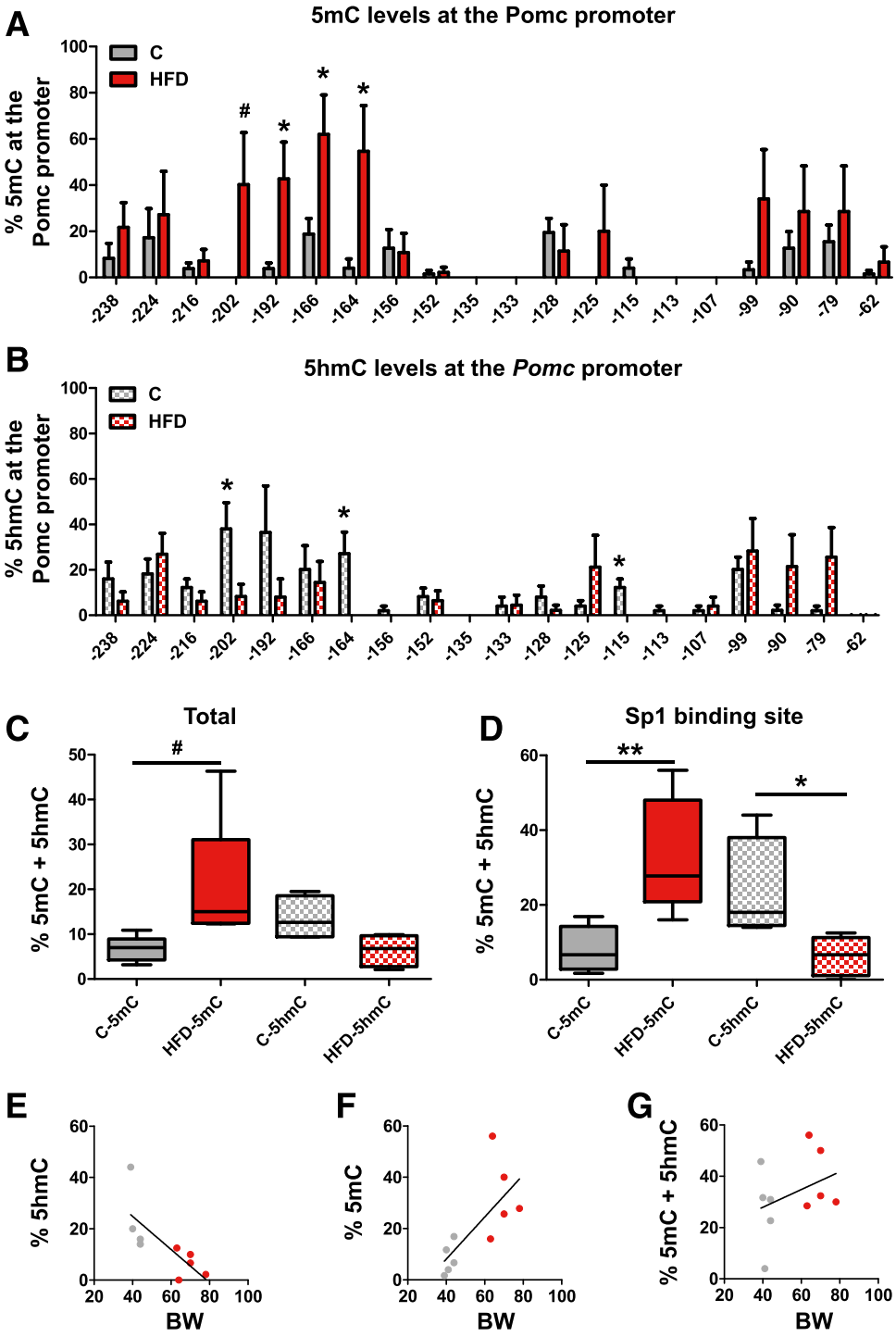

Figure 2—Specific regions that are essential for *Pomc* transcription are enriched with 5hmC and strongly depleted in 5mC in lean weaned offspring. Analysis of 5mC (*A*) and 5hmC (*B*) levels at the *Pomc* promoter in the hypothalamic ARC region in weaned offspring of either HFD-fed or chow-fed dams (HFD and C, respectively). The analyzed *Pomc* promoter region includes 20 CpG dinucleotides and functional regulatory elements that are critically involved in the transcription of *Pomc* and mediated through leptin signaling. Error bars represent the variance in the methylation percentage from each group. For the statistical analysis, differences in methylation patterns were analyzed by both exploratory χ^2 analyses and Student *t* test. The percentages of 5mC and 5hmC in each rat were calculated in the *Pomc* promoter in two regions: from −238 bp upstream of the transcriptional start site to +1 (total) (*C*) and from −192 to −133 bp region upstream of the transcriptional start site (Sp1 binding site) (*D*). Pearson product-moment correlations were performed for each rat among 5hmC (*E*), 5mC (*F*), and 5hmC + 5mC (*G*) levels of the −192 to −133 cluster and rat's BW. *C*, *n* = 5/group; HFD, *n* = 5/group, 12–17 clones/animal. All data are presented as means ± SEM. #$P < 0.1$, *$P < 0.05$, **$P < 0.01$ vs. control group.

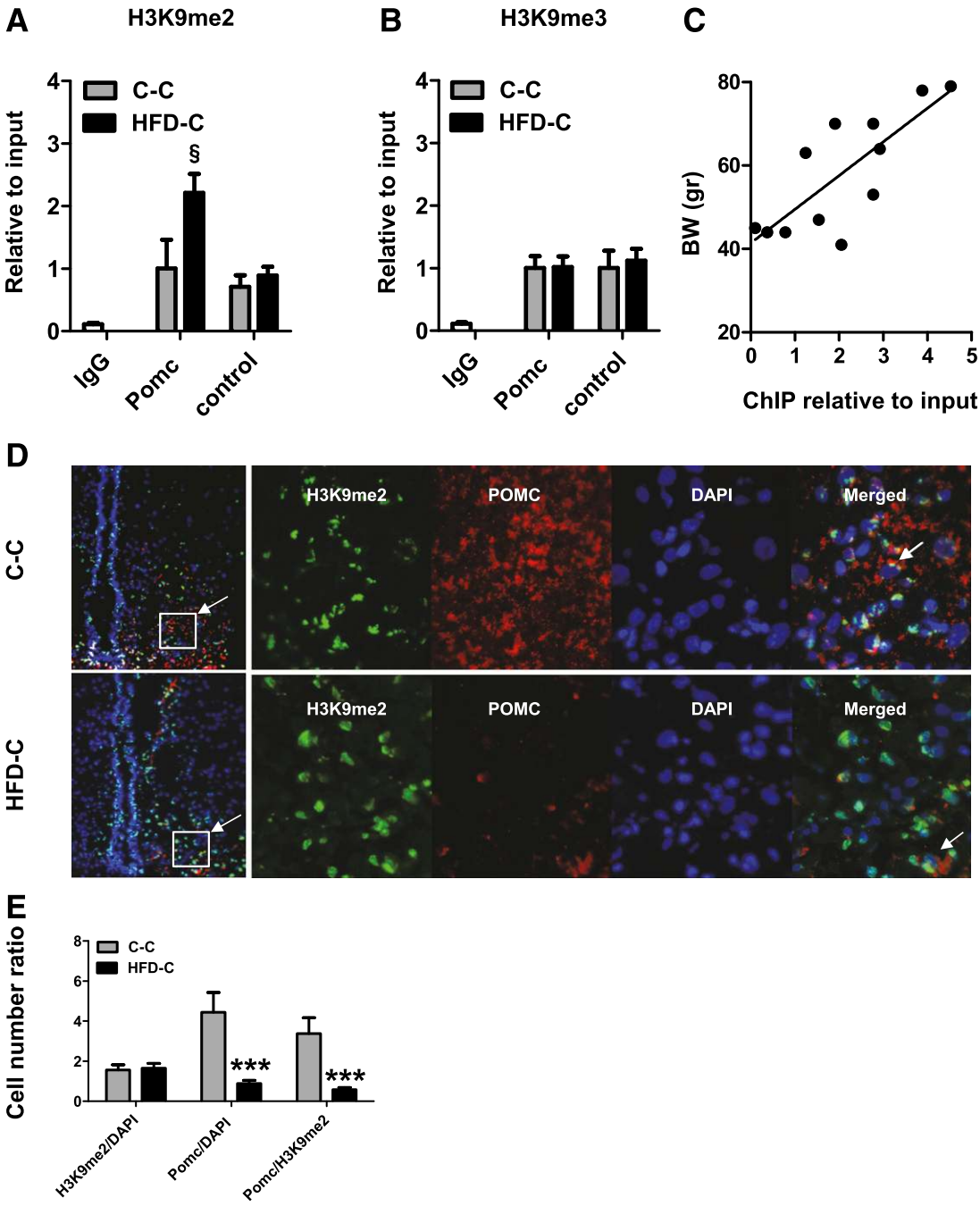

Figure 3—HFD-C present higher H3K9me2 levels at the *Pomc* promoter, specifically at the hypothalamic ARC nuclei, than C-C. ARC samples were immunoprecipitated with antibodies against H3K9me2 (*A*) or H3K9me3 (*B*) and subjected to real-time PCR with two sets of primers. *Pomc*: primers aligning at positions −318 to −28 bp upstream of the *Pomc* transcriptional start site. Control: primers aligning at nonrelevant positions +5615 to +5714 bp downstream of the transcriptional start site (exon 3). Immunoprecipitation with normal rabbit IgG was used as a negative control. C-C PCR abundance value was set to 1. $n = 6$/group. *C*: Pearson product-moment correlations were performed between the H3K9me2 or *Pomc* promoter levels of each rat and their BW. *D*: Immunofluorescent staining of frozen coronal brain sections of the hypothalamus. The sections were immunostained with anti-H3K9me2 or anti-POMC antibodies and DAPI. *E*: Quantification of the immunofluorescent staining. Four different sections were examined in each animal. Four different rats were analyzed per group. The number of stained cells was analyzed by ImageJ 1.3 image analysis software (National Institutes of Health). Data are presented as mean ± SEM. §$P < 0.05$, Bonferroni post hoc test vs. control; ***$P < 0.001$, Student *t* test vs. control group.

histone marks, binding levels of MeCP2 and MBD1 to the *Pomc* promoter were assessed (Fig. 4*A* and *B*). The ARC samples subjected to ChIP assay showed less MeCP2 binding to the *Pomc* promoter ($n = 5$, $F_{(2,12)} = 16.4$, $P = 0.003$ between groups; HFD-C versus C-C Bonferroni post hoc test, twofold, $P < 0.05$) (Fig. 4*A*). In addition, these

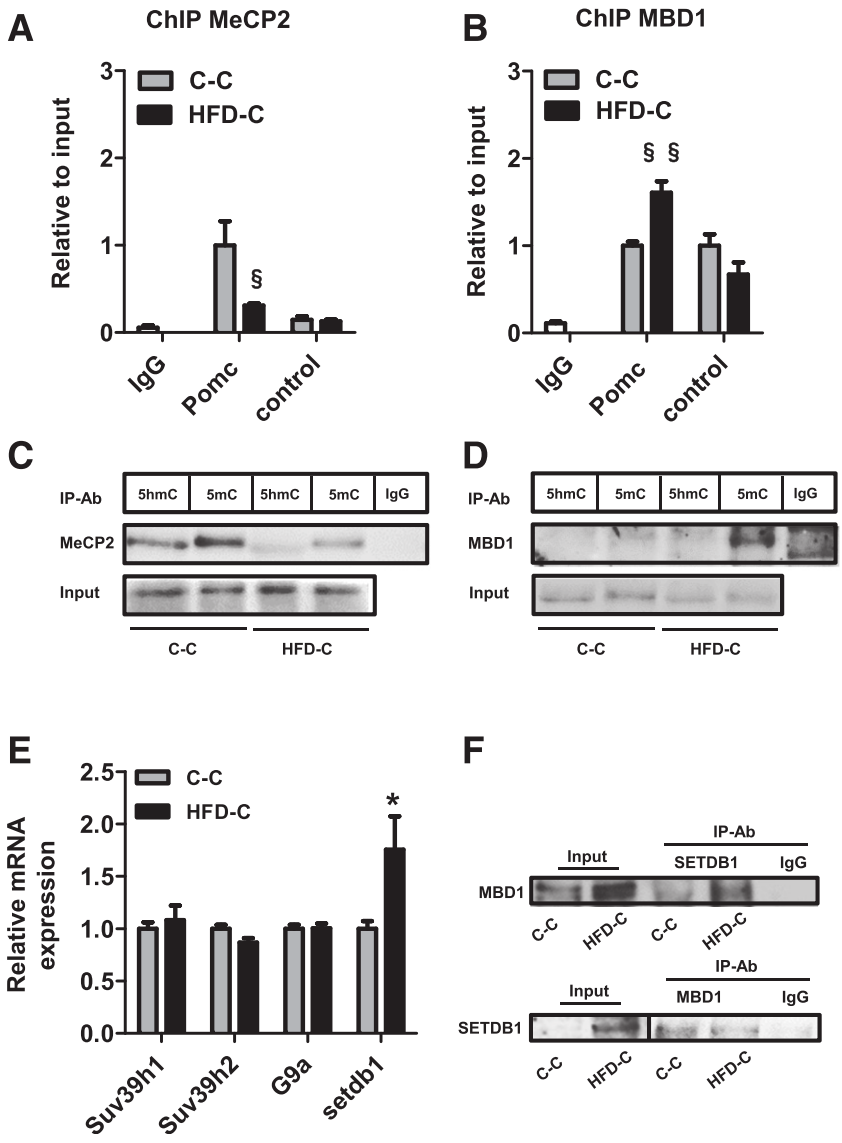

Figure 4—MBD1 binds to 5mC, but not 5hmC, at the *Pomc* promoter to promote inactive chromatin structure through H3K9 methyltransferase SETDB1. ARC samples were immunoprecipitated with antibodies against MeCP2 (*A*) or MBD1(*B*) and subjected to real-time PCR with two sets of primers. *Pomc*: primers aligning at positions −318 to −2 bp upstream of the *Pomc* transcriptional start site. Control: primers aligning at nonrelevant positions +5615 to +5714 bp downstream of the transcriptional start site (exon 3). Immunoprecipitation with normal rabbit IgG was used as a negative control. C-C PCR abundance value was set to 1. n = 6–8/group. ARC of C-C and HFD-C were subjected to co-IP assay with anti-5mC and anti-5hmC antibodies. Normal IgG served as negative control. IP proteins and input samples were separated and detected by Western blot analysis using antibodies against MeCP2 (*C*) or MBD1 (*D*) (due to different exposure times, the input and immunoprecipitated membranes were cut and exposed separately). *E*: C-C and HFD-C were sacrificed and analyzed for mRNA levels of *Suv39h1*, *Suv39h2*, *G9a*, and *Setdb1*. Relative gene expression in the C-C group was set to 1. *Hprt1* and *B2m* were used as standard genes. *D*: ARC samples of C-C and HFD-C were subjected to co-IP assays with anti-MBD1 and anti-SETDB1 antibodies. IP proteins and input samples were separated and detected by Western blot analysis using antibodies against SETDB1 or MBD1. The IP of both 5mC and IgG were performed using the same input. All data are presented as mean ± SEM. *P < 0.05, vs. C-C group by t test; §P < 0.05, §§P < 0.001, different from control group by Bonferroni post hoc test.

offspring presented higher MBD1 binding levels to the *Pomc* promoter in the HFD-C versus C-C (n = 5, $F_{(2,12)}$ = 7.4, P = 0.008 between groups; HFD-C versus C-C Bonferroni post hoc test, 1.7-fold, P = 0.002) (Fig. 4*B*). All groups differed from the level of the negative control IgG (P = 0.001). There were no changes in the binding levels of either MeCP2 or MBD1 at the control site. Next, we examined whether MBD1 or MeCP2 can merge into a complex with 5mC, 5hmC, or both marks together. Each sample from the ARC nuclei of C-C and HFD-C was precipitated with either 5mC or 5hmC antibody and blotted with MBD1/MeCP2 antibodies. MBD1 bound only to the 5mC modification in the HFD-C group, but failed to bind to the 5hmC derivative in any of the groups (Fig. 4*C*).

Moreover, MeCP2 was seen to interact with both 5mC and 5hmC marks, but the complexes were much more abundant in the C-C group (Fig. 4*D*).

Because MBD1 interacted only with the 5mC marks, we searched for the mechanism that links this modification and the histone marks. Given that MBD1 interacts with H3K9 methyltransferases to establish silent chromatin (4), we evaluated the expression of specific enzymes known as modifiers of this site—euchromatic histone lysine N-methyltransferase 2, SUV39H1 (Drosophila), SUV39H2, and SETDB1—in the offspring (9). Of the four enzymes tested, only SETDB1 showed higher mRNA levels in the HFD-C group than in the C-C group (n = 7, 1.7-fold, P = 0.039) (Fig. 4*E*). Hence, to test for an interaction between MBD1 and the SETDB1 complex, we subjected ARC nuclei from C-C and HFD-C to coimmunoprecipitation (co-IP) analysis (Fig. 4*F*). MBD1 coprecipitated with SETDB1 only in the HFD-C rats. Moreover, Western blot analysis showed that SETDB1 is present in all MBD1-immunoprecipitated samples. It is important to note that higher protein levels of MBD1 and SETDB1 in the input of the HFD-C group compared with that of the C-C group are due to their augmented expression in the HFD-C rats, as demonstrated by Western blot (Fig. 4*F*) and quantitative RT-PCR analysis (Fig. 4*E*), and not to a technical problem. Taken together, the results suggest that MBD1 offers an interactive surface for SETDB1 to implement the methylation modification on H3K9 at the *Pomc* promoter.

DISCUSSION

Impaired ability of leptin signaling to affect downstream physiological pathways in the brain results in persistent dysregulation of food intake and energy homeostasis (15). This disturbance might be mediated by epigenetic malprogramming, specifically via regulation of the expression of the anorexigenic polypeptide POMC. In this study, both postweaning rats chronically exposed to an HFD and offspring of HFD-fed dams developed hyperphagia, increased BW, and high levels of leptin and insulin. These elevated hormone levels are expected to increase the expression of *Pomc*, leading to increased energy expenditure and reduced BW (16,17). However, obese rats presented decreased levels of *Pomc* mRNA expression, indicating that the high levels of leptin did not affect *Pomc* expression adequately. DNA-CpG methylation analysis in these animals revealed hypermethylation in HFD-fed rats at specific transcription factor binding sites in the *Pomc* promoter that are associated with leptin signaling, probably blocking the anorexigenic actions of leptin (1–3). Nevertheless, although most offspring rapidly gained weight, some only gained as much weight as those fed a low-fat diet. This suggests that obesity proneness and resilience traits are regulated by different epigenetic codes, which might be mediated by 5hmC or 5mC.

Recent evidence has shown that 5hmC is a stable epigenetic mark, which, as opposed to 5mC, promotes gene expression and increases accessibility to chromatin structures. In this study, we used the oxidized bisulfite sequencing method (12) and showed higher 5hmC levels in specific clusters on the *Pomc* promoter of lean rats and a negative correlation with BW of individuals from both groups (Fig. 2). These results support the hypothesis that 5hmC is a stable mark in the brain (12,18) that might be associated with *Pomc* regulation. We note that a limitation of our approach lies in the fact that the analyses of both 5mC and 5mhC were performed on DNA that was extracted from a square millimeter punch of the ARC area, which contains many cell types, including neurons and glia, cells that belong to the feeding circuits, and others with different physiological roles. This combined cell population is bound to increase the variability in our results. Nevertheless, the fact that we identified DNA-methylation differences between feeding treatments increases the likelihood that indeed the described epigenetic mechanism underlies the differences between obesity and leanness in our samples.

There is accumulating evidence for the role of 5hmC marks in the regulation of chromatin architecture and gene transcription (19,20). In some instances, 5mC physically blocks the binding of a transcription factor to its target (21). Alternatively, by blocking the binding of repressors, methylation can increase the expression of a gene (22). It is unlikely that 5hmC would restore binding, because it is bulkier than 5mC and therefore might block the binding of proteins that tolerate 5mC (18). A second theory suggests that 5hmC strongly inhibits the binding of MBD proteins to the DNA and induces transcriptional activation (8,23). MBDs can recruit proteins such as HDACs (5), histone methyltransferases (14), and other chromatin-remodeling complexes known to promote the formation of a condensed chromatin structure. These findings suggest a role for a possible complex mediating the signals applied by 5mC marks to promote modifications of histones for gene regulation (14). Another possible mechanism of expression enhancement by 5hmC may be by preventing DNA methyltransferase recruitment, which also promotes (on its own) the recruitment of HDACs and H3K9 methyltransferases to DNA (18). In agreement with these theories, in this study, lean rats (C-C) that displayed higher 5hmC levels on the *Pomc* loci also presented lower levels of the repressive H3K9me2 marks (Fig. 3*A*) at the hypothalamic ARC nucleus (Fig. 4). In contrast, offspring of HFD-fed dams presented higher levels of H3K9me2 (Fig. 3*A*), accompanied by high 5mC levels and lower hypothalamic *Pomc* expression (Figs. 4 and 1*C*). The localization of these marks was confirmed by immunostaining, with HFD-C presenting a low H3K9me2/*Pomc* ratio (Fig. 3) in the ARC region of the hypothalamus.

Regarding the need for dual epigenetic silencing marks (i.e., both DNA and histone methylation), there is a growing body of evidence that indicates a synergy between the two. For example, DNA methyltransferases have been shown to interact with both the histone methyltransferase SUV39, which is responsible for methylation of H3K9, and

EZH2, which catalyzes H3K27 methylation (24). These interactions have been proven to be important for 5mC of heterochromatin and EZH2-targeted genes. DNA methyltransferases have also been shown to interact with heterochromatin protein 1, which specifically binds to methylated lysine 9 on histone 3, and they recruit DNA methyltransferases to loci marked by H3K9me3 (25). Further support for the notion that methylation of H3K9 and H3K27 may target 5mC comes from genome-wide studies showing that these histone modifications precede DNA methylation. These studies further showed that when DNA methylation is inhibited, there is no effect on the methylation of H3K9 or H3K27 in repeat sequences or CpG islands (26). The suggested mediation of the interaction between these two major epigenetic systems by different DNA-methyl derivatives, such as 5hmC, opens up new possibilities.

In this study, we describe a two-step mechanism that propagates the repression of *Pomc* gene expression, carried out by a synergistic alteration in DNA-methylation marks and histone PTM mediated by MBD1 and MeCP2. These mediators have been shown to serve as interacting surface anchors for the H3K9 methyltransferase enzymes, which promote repressive complexes on genes and condensed chromatin structure (4,9). MeCP2 has a complex regulatory role: it may bind to either 5hmC or 5mC marks, and it promotes both active and repressive gene expression (27). Nevertheless, in a mouse line with specific deletion of MeCP2 in the *Pomc* neurons, it was shown that MeCP2 positively regulates *Pomc* expression in the hypothalamus. Absence of MeCP2 in the POMC neurons led to increased DNA methylation of the *Pomc* promoter, which, in turn, downregulated *Pomc* expression, leading to obesity in mice (28). In agreement, our results showed that MeCP2 can bind to both 5mC and 5hmC derivatives (Fig. 4*C*). In addition, we found a twofold reduction of MeCP2 binding levels to the *Pomc* promoter site in lean offspring (C-C, Fig. 4*A*). Together with previous results, this implies that the MeCP2–5hmC interaction promotes active *Pomc* expression and that it may be protective to increased 5mC levels. In contrast, co-IP analyses with MBD1 showed that this mediator can bind only to the 5mC derivative (Fig. 4*D*). In addition, MBD1 binding to the promoter site of *Pomc* was higher in the HFD-C (Fig. 4*B*). These results are in agreement with reports that MBD1 binds exclusively to 5mC marks (29). The repressive mechanism of MBD1 may involve deacetylation, as the deacetylase inhibitor trichostatin A can partly overcome the repression (30). Moreover, MBD1 also presents an interacting surface for the methyltransferase enzymes (14,24).

Because our data indicated that obese rats have elevated methylation levels of H3K9 in the *Pomc* promoter area, we studied H3K9 methylase enzymes. Among the four enzymes examined, HFD-C rats only showed higher levels of *Setdb1* mRNA expression. In agreement, co-IP analysis revealed that MBD1 forms a stable complex with SETDB1 methyltransferase. Collectively, these findings suggest a possible complex that links DNA methylation and histone PTMs and contributes to our understanding of the mechanisms

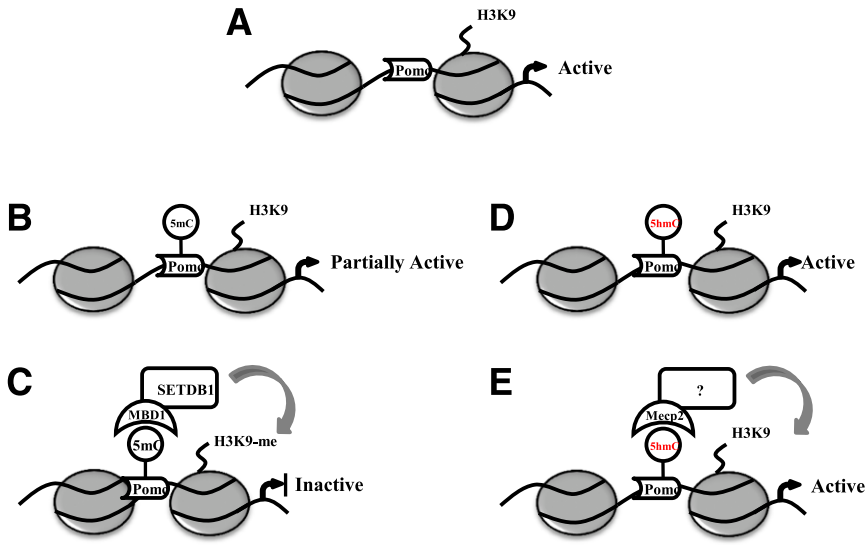

Figure 5—Diagram of potential epigenetic repression mechanism regulating POMC expression in diet-induced obesity. *A*: Under normal conditions, *Pomc* is fully accessible to the transcription mechanisms mediated by hormonal signals, such as leptin. *B*: DNA-CpG methylation on the promoter of *Pomc* interferes with the transcription mechanisms, leading to only partial activation of the gene. *C*: A repressor complex including binding of MBD1 to the DNA-CpG methylated site on the *Pomc* promoter. MBD1 interacts with SETDB1 methyltransferase to promote methylation of H3K9. *D*: 5hmC is enzymatically produced by a stepwise oxidation of 5mC by the ten-eleven translocation family dioxygenases. *E*: 5hmC inhibits the binding of MBD1, disrupting the formation of a repressive complex at the CpG sites. Instead, other chromatin modulators, such as Mecp2, interact with 5hmC to promote open chromatin structure and increased POMC response to high-energy signals. These results suggest a possible epigenetic regulatory complex that links DNA methylation and histone PTMs at the *Pomc* promoter.

through which environmental cues are translated into stable changes ("cellular memory") in the *Pomc* gene. In our proposed model (Fig. 5), under maternal HFD environmental conditions, MBD1 binds to the 5mC derivative and recruits SETDB1 methyltransferase. This enzyme promotes methylation on K9 of H3 and forms a dual silencing complex on the *Pomc* promoter, which leads to reduced satiety, increased caloric intake, overweight, and obesity. More importantly, in the presence of the 5hmC mark, MBD1 cannot bind to the CpG sites, allowing for an open chromatin structure and increased response of *Pomc* to energy-storage signals. Thus, the interplay between these two epigenetic marks potentially allows for diverse individual profiles of more or less resistance/susceptibility to the environmental pressure of a maternal HFD.

Funding. This research was supported by the Israel Science Foundation (grant 1532/12) and the Israel Poultry Board (grant 356065414).

Duality of Interest. No potential conflicts of interest relevant to this article were reported.

Author Contributions. A.M. planned the study (with A.W. and N.M.), performed the research, analyzed the data, and wrote the first draft of the manuscript. T.K. assisted in the research and data analysis and trained the team on some of the methods. T.T. assisted in performing the research. A.W. planned experiments, assisted in data analysis, and reviewed and edited the manuscript. N.M. planned and supervised the experiments and reviewed and edited the manuscript. A.W. and N.M. are the guarantors of this work and, as such, had full access to all the data in the study and take responsibility for the integrity of the data and the accuracy of the data analysis.

Prior Presentation. This study was presented at the 2016 Obesity Summit, London, U.K., 12–14 April 2016.

References

1. Marco A, Kisliouk T, Weller A, Meiri N. High fat diet induces hypermethylation of the hypothalamic Pomc promoter and obesity in post-weaning rats. Psychoneuroendocrinology 2013;38:2844–2853
2. Plagemann A, Harder T, Brunn M, et al. Hypothalamic proopiomelanocortin promoter methylation becomes altered by early overfeeding: an epigenetic model of obesity and the metabolic syndrome. J Physiol 2009;587:4963–4976
3. Zhang X, Yang R, Jia Y, et al. Hypermethylation of Sp1 binding site suppresses hypothalamic POMC in neonates and may contribute to metabolic disorders in adults: impact of maternal dietary CLAs. Diabetes 2014;63:1475–1487
4. Kouzarides T. Chromatin modifications and their function. Cell 2007;128:693–705
5. Miranda TB, Jones PA. DNA methylation: the nuts and bolts of repression. J Cell Physiol 2007;213:384–390
6. Song CX, Yi C, He C. Mapping recently identified nucleotide variants in the genome and transcriptome. Nat Biotechnol 2012;30:1107–1116
7. Kellinger MW, Song CX, Chong J, Lu XY, He C, Wang D. 5-formylcytosine and 5-carboxylcytosine reduce the rate and substrate specificity of RNA polymerase II transcription. Nat Struct Mol Biol 2012;19:831–833
8. Mellén M, Ayata P, Dewell S, Kriaucionis S, Heintz N. MeCP2 binds to 5hmC enriched within active genes and accessible chromatin in the nervous system. Cell 2012;151:1417–1430
9. Day JJ, Sweatt JD. Epigenetic treatments for cognitive impairments. *Neuropsychopharmacology* 2012;37:247–260
10. Bouret SG, Simerly RB. Developmental programming of hypothalamic feeding circuits. Clin Genet 2006;70:295–301
11. Fan C, Liu X, Shen W, Deckelbaum RJ, Qi K. The Regulation of Leptin, Leptin Receptor and Pro-opiomelanocortin Expression by N-3 PUFAs in Diet-Induced Obese Mice Is Not Related to the Methylation of Their Promoters. Nutr Metab (Lond) 2011;8:31
12. Booth MJ, Branco MR, Ficz G, et al. Quantitative sequencing of 5-methylcytosine and 5-hydroxymethylcytosine at single-base resolution. Science 2012;336:934–937
13. Marco A, Kisliouk T, Tabachnik T, Meiri N, Weller A. Overweight and CpG methylation of the Pomc promoter in offspring of high-fat-diet-fed dams are not "reprogrammed" by regular chow diet in rats. FASEB J 2014;28:4148–4157
14. Fujita N, Watanabe S, Ichimura T, et al. Methyl-CpG binding domain 1 (MBD1) interacts with the Suv39h1-HP1 heterochromatic complex for DNA methylation-based transcriptional repression. J Biol Chem 2003;278:24132–24138
15. Tups A. Physiological models of leptin resistance. J Neuroendocrinol 2009; 21:961–971
16. Cowley MA, Smart JL, Rubinstein M, et al. Leptin activates anorexigenic POMC neurons through a neural network in the arcuate nucleus. Nature 2001; 411:480–484
17. Cone RD, Lu D, Koppula S, et al. The melanocortin receptors: agonists, antagonists, and the hormonal control of pigmentation. Recent Prog Horm Res 1996;51:287–317; discussion 318
18. Pastor WA, Aravind L, Rao A. TETonic shift: biological roles of TET proteins in DNA demethylation and transcription. Nat Rev Mol Cell Biol 2013;14:341–356
19. Kaas GA, Zhong C, Eason DE, et al. TET1 controls CNS 5-methylcytosine hydroxylation, active DNA demethylation, gene transcription, and memory formation. Neuron 2013;79:1086–1093
20. Valinluck V, Tsai HH, Rogstad DK, Burdzy A, Bird A, Sowers LC. Oxidative damage to methyl-CpG sequences inhibits the binding of the methyl-CpG binding domain (MBD) of methyl-CpG binding protein 2 (MeCP2). Nucleic Acids Res 2004; 32:4100–4108
21. Yossifoff M, Kisliouk T, Meiri N. Dynamic changes in DNA methylation during thermal control establishment affect CREB binding to the brain-derived neurotrophic factor promoter. Eur J Neurosci 2008;28:2267–2277
22. Bell AC, Felsenfeld G. Methylation of a CTCF-dependent boundary controls imprinted expression of the Igf2 gene. Nature 2000;405:482–485
23. Hashimoto H, Liu Y, Upadhyay AK, et al. Recognition and potential mechanisms for replication and erasure of cytosine hydroxymethylation. Nucleic Acids Res 2012;40:4841–4849
24. Fuks F, Hurd PJ, Deplus R, Kouzarides T. The DNA methyltransferases associate with HP1 and the SUV39H1 histone methyltransferase. Nucleic Acids Res 2003;31:2305–2312
25. Smallwood A, Estève PO, Pradhan S, Carey M. Functional cooperation between HP1 and DNMT1 mediates gene silencing. Genes Dev 2007;21:1169–1178
26. McGarvey KM, Fahrner JA, Greene E, Martens J, Jenuwein T, Baylin SB. Silenced tumor suppressor genes reactivated by DNA demethylation do not return to a fully euchromatic chromatin state. Cancer Res 2006;66:3541–3549
27. Kriaucionis S, Tahiliani M. Expanding the epigenetic landscape: novel modifications of cytosine in genomic DNA. Cold Spring Harb Perspect Biol 2014; 6:a018630
28. Wang X, Lacza Z, Sun YE, Han W. Leptin resistance and obesity in mice with deletion of methyl-CpG-binding protein 2 (MeCP2) in hypothalamic pro-opiomelanocortin (POMC) neurons. Diabetologia 2014;57:236–245
29. Yildirim O, Li R, Hung JH, et al. Mbd3/NURD complex regulates expression of 5-hydroxymethylcytosine marked genes in embryonic stem cells. Cell 2011; 147:1498–1510
30. Ng HH, Jeppesen P, Bird A. Active repression of methylated genes by the chromosomal protein MBD1. Mol Cell Biol 2000;20:1394–1406